



Effect of Soldering Temperature on the Reliability of Sn-Ag-Cu Lead-Free Solder Joints

ZHAI XINMENG,¹ LI YUEFENG ,^{1,2} ZOU JUN,^{1,3} SHI MINGMING,¹
YANG BOBO,¹ LI YANG,¹ GUO CHUNFENG,¹ and HU RONGRONG¹

1.—College of Science, Shanghai Institute of Technology, Shanghai 201418, People's Republic of China. 2.—e-mail: yf_li@sit.edu.cn. 3.—e-mail: zoujun@sit.edu.cn

This paper investigates the effect of soldering temperature on solder joint voids and reliability of flip-chip LED chips during reflow soldering. Lead-free solder SAC305 was used as solder paste. The void ratio of the flip-chip LED solder joint at 250°C, 260°C, 270°C, 280°C, and 290°C reflow soldering temperatures was detected by x-ray detector. Shear tests were conducted to evaluate the influence of interfacial reactions on the mechanical reliability of solder joints. The distribution of voids in the shear section was observed by scanning electron microscope (SEM). Next, the photoelectric and thermal properties of FC-LED filament were tested and analyzed. Finally, a high-temperature and high-humidity aging experiment was carried out to test the reliability of the LED filament. The results show that the void ratio of the LED filament soldering joint is the lowest when the soldering temperature is 270°C. The small void ratio of the solder joints results in lower steady-state voltage and junction temperature of the flip-chip LED filament. As the void density in the solder joint decreases, the shear strength of the solder joint increases. At this time, the shear resistance and mechanical reliability are the highest.

Key words: Flip-chip LED chip, soldering temperature, voids, SEM, reliability

INTRODUCTION

The flip-chip LED chip technology not only overcomes the shortcomings of the LED chip, but also improves the reliability and life of LED products (Fig. 1). Because of its excellent characteristics in photo-thermal-electricity, it has been widely developed and applied in the field of lighting. In the actual production process, the soldering process is a key step in the flip-chip packaging process. The reliability of the flip-chip mounting solder joint is considered to be one of the most important reliability issues, which seriously affects its heat

dissipation, mechanical support and electrical conductivity performance.^{1–6}

High soldering temperature may cause a series of problems, including oxidation and yellowing of substrate materials, and thermal damage to chips. The soldering temperature and cost of Sn-3.0Ag-0.5Cu (SAC305) solder alloy are lower compared with gold-tin eutectic solder alloys (such as Au80Sn20).^{7–9} Therefore, it has been widely used as a die attach material for flip-chip LEDs. However, the existence of voids in the chip connection solder joint has been considered to be one of the main problems causing chip-level reliability problems on the substrate in microelectronics and optoelectronic devices. Although the standard IPC-A610F indicates that the allowable void ratio is less than 40%, a void ratio below 40% can also cause package failure, especially under severe application

(Received September 30, 2020; accepted December 18, 2020; published online January 12, 2021)

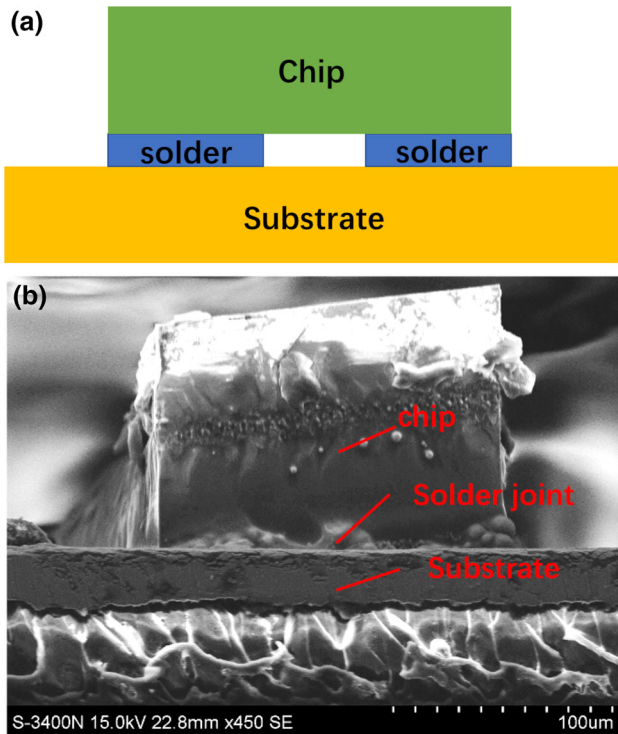


Fig. 1. Flip-chip LED package structure: (a) model diagram (b) package cross-sectional diagram.

conditions. Previous studies have shown that the degassing of organic tin paste during the reflow soldering process is the main reason for the formation of voids in the manufacturing stage. Sun and Zhang¹⁰ concluded that mechanical properties are one of the important features for evaluating the reliability of solder joints. In addition, the chip is the main contributor to the overall heat distribution of the packaged device. The increasing void rate will reduce the heat dissipation efficiency in the chip mount solder joint, because it will reduce the effective heat transfer area. The continuous increase of the void ratio will reduce the effective heat transfer area, which leads to an increase in the LED junction temperature,¹¹ thereby reducing the heat dissipation efficiency in the solder joint. The entire LED package usually fails due to overheating of the chip. Ciampolini et al.¹² concluded that the existence of large voids significantly reduces the service life of the package, while multiple small voids accelerate the failure process of the package, especially when they are close to the chip side. Chengshuo et al.¹³ studied the mechanical and thermal properties of SAC305 solder joint with arbitrary voids in high-power LED CSP through finite element simulation and experiment. The results show that the size and location of the voids in the solder joint are the two biggest factors that affect the mechanical and thermal properties of the solder joints. Yang Liu et al.¹⁴ studied the influence of the percentage of voids in the solder joint on the shear strength and thermal properties through

experiments and finite element simulations. The results show that the increase in solder paste volume significantly reduces the void ratio in the solder joint, which improves the shear strength of the package. And a package with a lower porosity shows a lower junction temperature. Hailong et al.¹⁵ studied the effect of copper grain size on the formation of voids at the interface of SAC305 (Sn3.0Ag0.5Cu)/Cu solder joints. The results show that increasing the grain size reduces the tendency to form voids at the interface. Bušek et al.¹⁶ studied the large and micro-holes in the solder joints and the negative impact of the use of additional flux on the reliability of the solder joints. The results show that the void ratio can be significantly reduced by using an appropriate amount of appropriate flux in the solder paste, especially the flux with higher activity.¹⁷ However, there are few studies on the influence of voids on the mechanical, photoelectric and thermal properties of the soldering joint of flip-chip LED chips under different soldering temperatures.¹⁸

In this research, the mechanical properties, photoelectric and thermal properties of flip-chip LED filaments are studied at 250°C, 260°C, 270°C, 280°C, and 290°C reflow soldering temperature. The effect of voids on the solder joints of flip-chip LED chips is analyzed by x-ray and scanning electron microscope (SEM), and the best soldering temperature was compared. Finally, reliability aging verification was carried out.

SAMPLE PREPARATION AND TESTING

Sample Preparation

First, the blue film flip-chip LED chip is expanded by a crystal expander. The chip spacing is enlarged to facilitate the automatic grasping operation of the chip by the die bonder. The expanded flip-chip LED chip is fixed on the substrate with an ASM-AD860 die-bonding machine through lead-free solder according to the die-bonding process. The cross-sectional view of the flip-chip LED chip package is shown in Fig. 1, from top to bottom: chip, solder joint, and substrate. Then, the LED filaments were placed in the TORCH RS220 + (TORCH, Beijing,

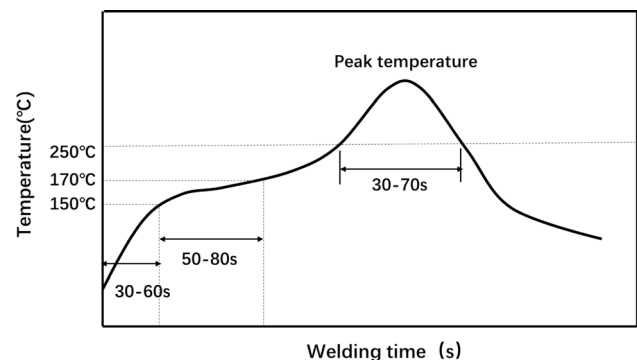


Fig. 2. Reflow soldering temperature curve of flip chip LED chip.

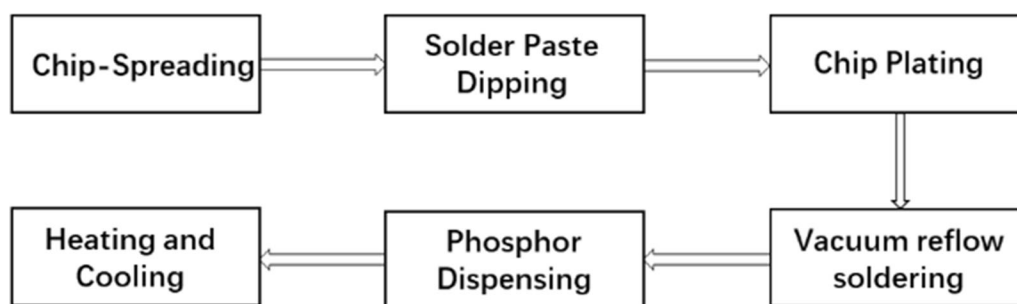


Fig. 3. Flip-chip LED packaging process.

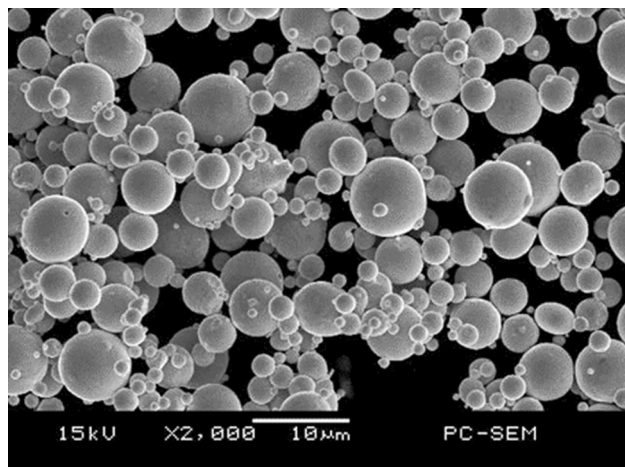


Fig. 4. SEM morphology of SAC305 lead-free solder paste.

China) type vacuum soldering furnace, the temperature was separately raised to 250°C, 260°C, 270°C, 280°C, 290°C after vacuum. The reflow soldering temperature curve is shown in Fig. 2 and the soldering time was 25 min. The soldering process of the chip is shown in Fig. 3.

Among them, Enraytek EA0820A (Enraytek, Shanghai, China) were used as flip-chip LED chips. P pole (positive polarity) and N pole (negative polarity) whose material is gold are located on the upper surface. The size of the chip was 8 mil × 20 mil, the working voltage was 3.1–3.2 V, and the wavelength was 452.5–455.0 nm. Moreover, Sn-3.0Ag-0.5Cu (SAC305) solder (Earlysun, Shenzhen, China) was used as solder paste, the main components are Sn-3.0Ag-0.5Cu and flux, and the melting point of the solder is 217–220°C. The thermal conductivity of SAC305 alloy is about 54–58 W/M K, and the microstructure of the alloy is shown in Fig. 4. The solder paste is placed at room temperature (about 25°C) to reheat for 1–2 h before use. A flexible substrate with a copper conductive joint is used as the substrate, with a thickness of 2 mm and a length of 175 mm. The number of chips for each LED filament is 100, and the rated voltage required for a single LED filament is 130 V.

Sample Test

One LED filament was randomly selected from the five groups of samples, the push–pull force required when any 20 chips on each substrate are pushed apart is tested using a XYZTEC strength tester (XYZTEC, Shenzheng, China). And x-ray is used to detect the void ratio of the soldering joint. Scanning electron microscope (SEM) is used to observe the size and position distribution of voids on the section. Five LED filaments were randomly selected from each of the five groups and lit with a constant current source of 285 V/15 mA, and the LED filament was defined as steady-state after 15 min of continuous lighting. The voltage and the luminous flux of the LED filament were measured by an LED300E (EVERFINE, Hangzhou, China) integration sphere, respectively. The junction temperature of the FC-LED LED filament was measured at room temperature 0 groups and lit with a constant current source of 285 V/15 mA using the LED-T300B thermal analysis system (LEETS, Shanghai, China). The FC-LED LED filament is aged at 85°C/85% relative humidity (RH) using GDJS-100 (Hangzhou, Hangzhou, China) high-temperature and high-humidity aging equipment. The steady-state voltage, blue light flux and junction temperature of the five groups of LED filaments were tested when they were aged for 100 h, 200 h, 300 h, 400 h, 500 h, and 600 h.

RESULTS AND DISCUSSION

By using the above test methods in turn, the void ratio of the solder joint and the SEM image of the shear section are detected.^{19,20} The box graph of the LED filament shear force, the broken line graph of the LED filament steady-state voltage, blue light flux and junction temperature, and the broken line graph of steady-state voltage and blue light flux with aging time are obtained. By summarizing and analyzing the above data, the influence of soldering temperature on solder joint void and reliability of flip-chip LED chips is obtained, and the best soldering temperature is finally obtained through comparison.

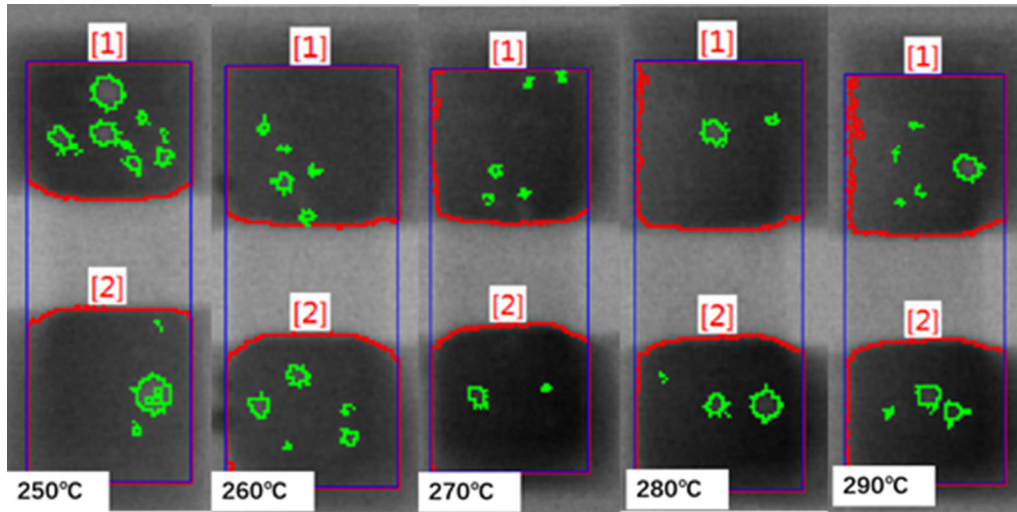


Fig. 5. X-ray detector detection images of the soldering joint of the LED filament under different soldering temperatures.

Table I. Void rate of LED filament solder joints at different soldering temperatures

Welding temperature	250°C	260°C	270°C	280°C	290°C
Average void rate	4.3%	2.9%	1.3%	3.5%	3.6%
Maximum void rate	9.2%	4.6%	2.8%	6.1%	6.0%

Void Detection of Solder Joints of Flip Chip LED Chips

Early studies have shown that x-ray is an effective non-destructive inspection method for voids and cracks in solder joints. Tian Tian et al.²¹ studied the vacancy flux in the SnPb solder joints of eutectic chips driven by electromigration using synchrotron radiation x-ray photomicrography, and quantitatively measured the changes in the void volume and shape in the three-dimensional image. Lei Su et al.¹⁰ reviewed and emphasized the main research results in the field of solder joint defect detection, including x-ray detection technology, and clarified the principle of the method and the corresponding advantages and disadvantages. There are two basic formation mechanisms of voids: First, the solder paste is mixed with the flux and powder of the solder alloy, and the flux is volatilized and melted during the reflow process. In this process, the gaps between the solder particles merge and form voids.²² Some voids will disappear from the molten solder, but other voids will remain and become voids in the solder joint. Secondly, when the chip is pressed on the substrate with solder paste and the solder paste is insufficient, a part of the gap appears in the solder paste, thereby forming a large gap after reflow.²³

Figure 5 shows the x-ray inspection image of the welded joint after the shear test. The x-ray detector is used to detect the void condition of the device, and the void rate is automatically calculated by the

instrument.²⁴ When the soldering temperature is 270°C, the void rate of the solder joint is significantly lower, the average void rate is less than 1.3%, and the maximum void rate is 2.8%. For other soldering temperatures, the average void rate of the solder joint is 3.7%, and the maximum void rate is as high as 9.2%. The IPC-A-610D standard further clarifies the specifications regarding the acceptable amount of voids in solder joints.²⁵ The IPC-7095 standard stipulates that the maximum allowable void area of Class II components is 25%.²⁶ Although they meet the requirements, the existence of voids in the soldering joint easily leads to an increase in the junction temperature and thermal resistance of the flip-chip LED chip, which in turn causes the photoelectric performance of the chip to decrease (Table I).²⁷

It can be seen from Fig. 5 that at 250°C and 260°C soldering temperatures, the void ratio of the solder joints is the highest, and most of them are large voids.²⁸ Large voids are considered process-related voids because they are generated during the manufacturing process (Fig. 6). This is because the soldering temperature is too low, and the air bubbles and volatilized flux gas do not completely overflow during the reflow soldering process of the chip soldering joint. Salleh et al.²⁹ studied the formation of solder voids, including how voids are formed and grow during the soldering process, especially in SAC solder joints. When the soldering temperature is 280°C and 290°C, the void ratio is relatively high. This is because the soldering

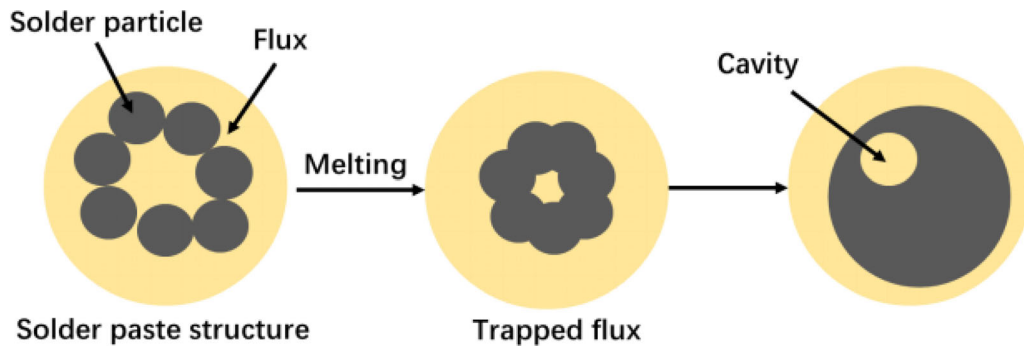


Fig. 6. Formation of large voids.

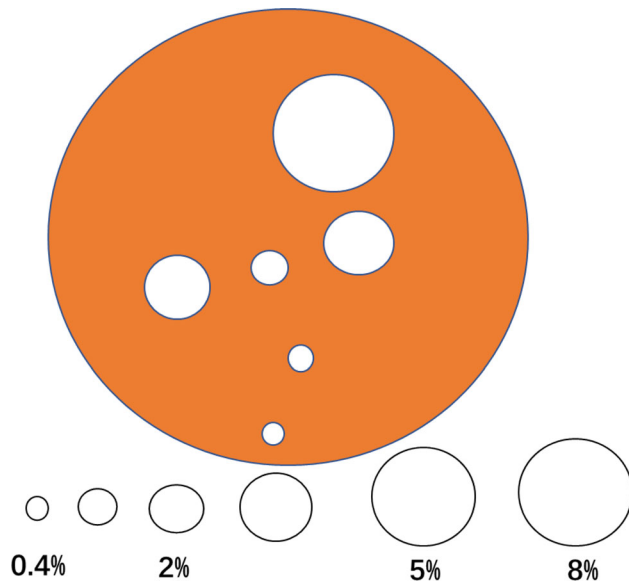


Fig. 7. Calculation method of solder joint void.

temperature is too high and the soldering time is short. The flux in the solder paste is heated and quickly evaporates before the elements form compounds, resulting in the thickness of the IMC joint uneven and large holes appear. The void that is too large will reduce the chip's shearing force.^{30,31} The research of Goyal et al.³² showed that the solder joints are more concentrated, which leads to the increased brittleness of Kirkendall void joints. Yunus et al.³³ concluded that a large void, regardless of its location, will significantly shorten the life of the joint. When there is a small cavity on the component side, it will accelerate the propagation of the crack. Due to the physical structure of solder paste, it is inevitable that there will always be voids in the joints made with solder paste. At a soldering temperature of 270°C, the voids of the solder joints are the lowest, and most of them are small voids with relatively uniform distribution. The opinions of soldering experts believe that small and evenly dispersed voids are an essential part of the joint.³⁴ The question of whether and how to avoid affecting the reliability of solder joints is still under discussion. The voids may act as stress relief and crack

arresters, and they can also become stress increasers. They can be located anywhere in the solder joint, and their location has a greater impact on reliability than their size. Even distribution of small voids in the joint cavity can appropriately increase its mechanical reliability.^{35,36}

Figure 7 shows how to calculate the area of the void. The void area expressed as area percentage is classified and then added together to obtain the total void area percentage. For example, there is a void of 0.4% (compared to the area of the solder joint), two voids of 2%, two voids of 5% and one void of 8% in Fig. 7, so the total void area is 22.4% (0.4% + 2 * 2% + 2 * 5% + 8%). Table II is the international gap classification standard (IPC-7095B).³⁷

The factors affecting the number of voids in a solder joint are shown in Fig. 8. Previous studies have shown that the reflow process and solder material are the most important factors affecting void formation. The impact of voids on solder joint reliability depends not only on size, but also on frequency and location. The location and size of the void may be a key factor affecting the performance and reliability of the solder joint. Due to the existence of bubbles, the high void rate will cause the thermal conductivity of the solder joint to decrease. Conductive heat transfer through solder joints can be modeled based on Fourier's law as follows:

$$Q = KA(T_1 - T_2)/L \quad (1)$$

where Q is the heat transfer, K is the thermal conductivity, A is the cross-sectional area of the solder joint, L is the length of the solid element, and T_1 and T_2 are the temperature of the source and receiver.

It can be seen from the above formula that the heat transferred is proportional to the cross-sectional area. The solder joints with voids can have a larger diameter to maintain the same volume in the solder joints. However, the cross-sectional area may be the same or different. The area of solder joints with voids may be small, which may interrupt heat flow.

Table II. Classification of gaps in IPC-7095B

	Class 1	Class 2	Class 3
Voids after SMT	Up to 70% balls may have voids. Maximum void size in any ball is 20% of area (45% of the image diameter) Balls with cumulative voids smaller than 4% of the area (20% of the image diameter) are not counted	Up to 60% balls may have voids. Maximum void size in any ball is 15% of area (40% of the image diameter)	Up to 50% balls may have voids. Maximum void size in any ball is 10% of area (32% of the image diameter)

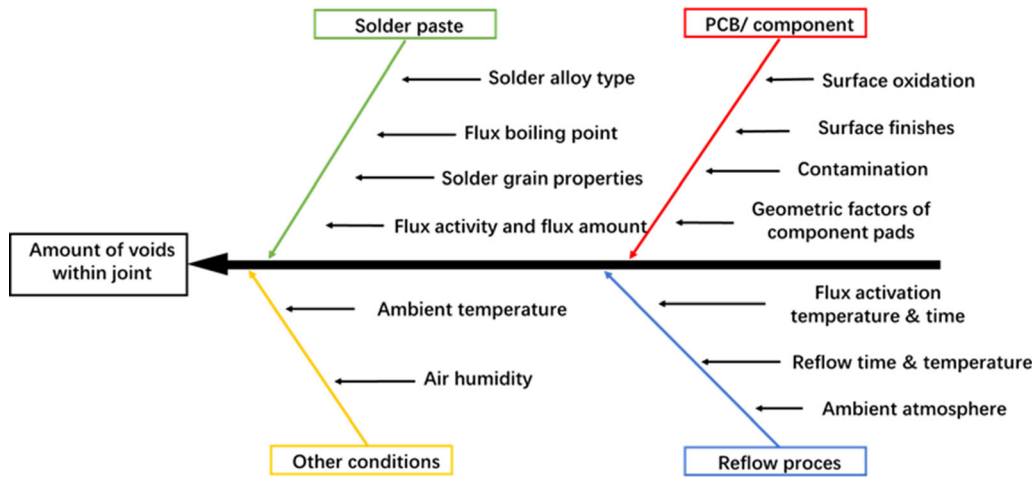


Fig. 8. Factors affecting the number of voids in a solder joint.¹⁶

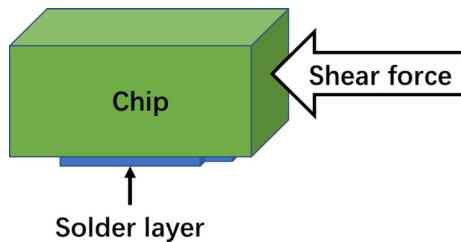


Fig. 9. The shear force applied to the test sample during the test.

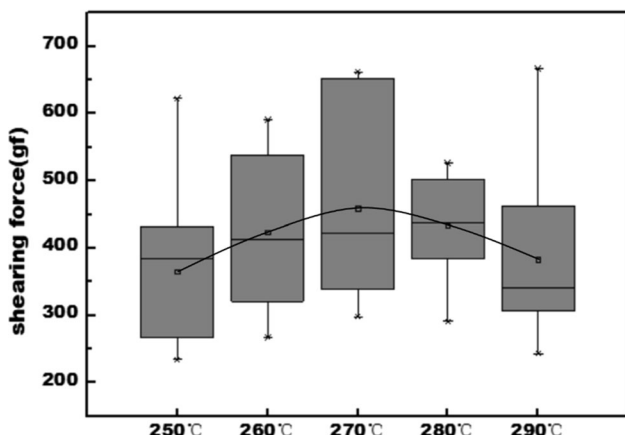


Fig. 10. Soldering temperature-average shear force box diagram.

Analysis of Chip Average Shear Force Under Different Soldering Temperatures

Shear tests were conducted to evaluate the influence of interfacial reactions on the mechanical reliability of solder joints (Fig. 9). Figure 10 shows the shear force of FC LED filament solder joints at different soldering temperatures. The shear force of the solder joints exceeds 200 gf (standard shear force). The average shear force of the solder joints at the five soldering temperatures is about 365.53 gf, 424.13 gf, 459.47 gf, 433.53 gf, and 383.20 gf, respectively. As the void density in the solder joint decreases, the shear strength of the solder joint increases. The shear fracture of these samples was observed by SEM, and the morphology is shown in Fig. 11. Since the bonding strength of the solder joint is related to the area, the reduction of the connection area and the large voids between the solder joints result in a decrease in strength. In addition, voids in the solder joint can cause stress concentration, and these stress concentration locations are the initial part of the crack under environmental load.³⁸ Generally, shear force has been used as a unit representing the mechanical reliability of solder joints. The peak shear stress is equal

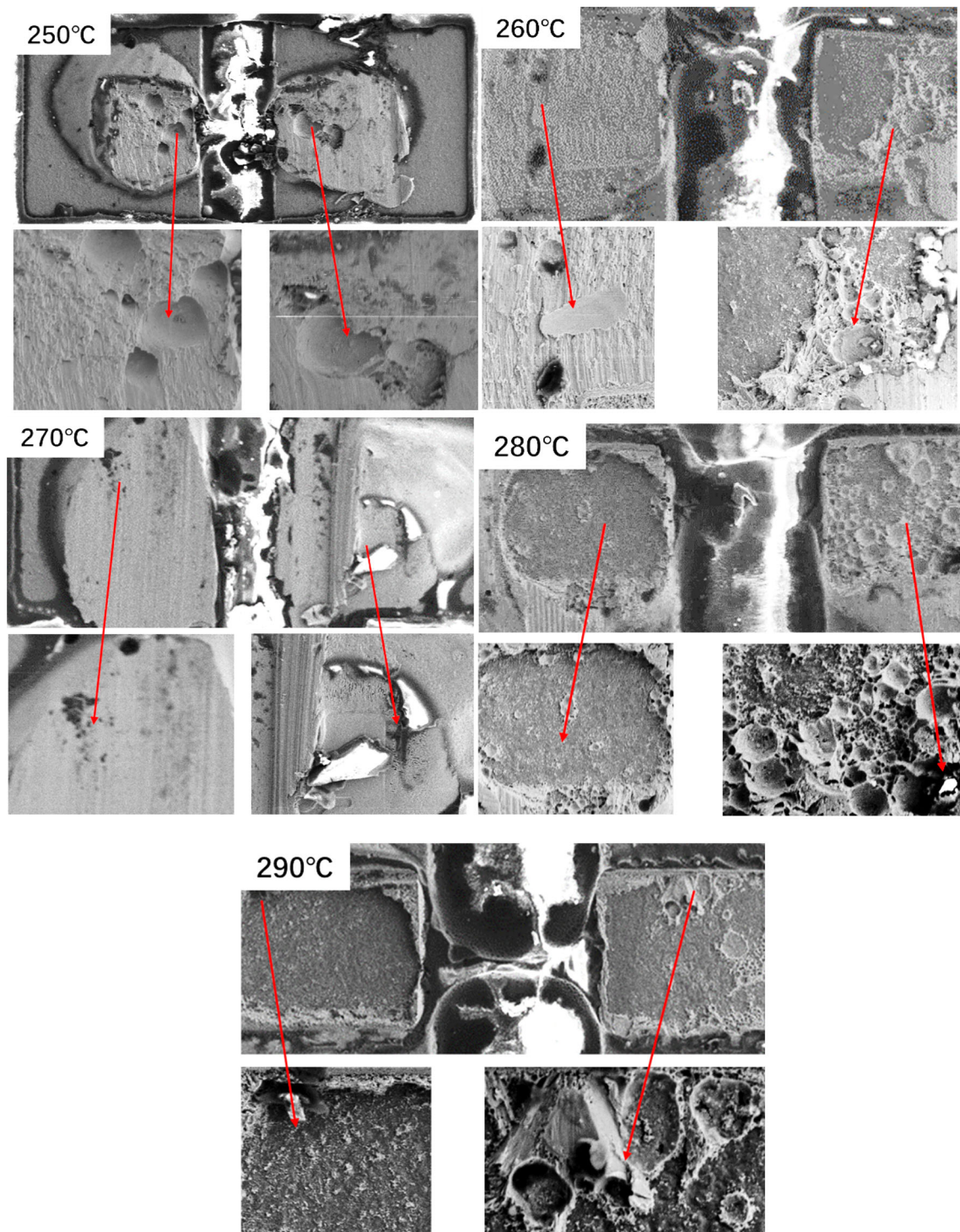


Fig. 11. SEM morphology of shear fracture surface.

to the peak shear force divided by the pad area of the substrate.³⁹

Figure 11 shows the SEM morphology of the shear fracture surfaces of five samples. Among them, when the soldering temperature is 270°C, the smooth morphology of the solder joint section indicates that an acceptable connection between the solder joint and the pad alloy has been achieved in

this area. The high shear strength of this sample type is mainly due to the small void area in the solder joint and the large effective contact area of the solder joint. When the soldering temperature is 250°C, the void ratio is the highest. This is because the soldering temperature is too low, which causes the flux in the solder joint to not volatilize in time, and eventually becomes void. The tiny grains in the

picture are the intermetallic compound (IMC) grains between the SAC305 and the Cu substrate. Obviously, a connection has been established in this area. However, the growth of the IMC joint is limited by the voids in the solder alloy. Although the set temperature has reached the melting point of the solder paste, most of the solder has not completely melted and still exists in the form of particles, and the elements at the chip-solder-substrate interface are not fully reacted. C.M.T. et al.⁴⁰ studied the thickness of the intermetallic joint (IML) formed between the solder and the Cu substrate immediately after soldering and after thermal aging at 170°C for 1000 h. It was found that the size of Sn grains was reduced and the wetting behavior was improved due to the addition of rare earth elements. When the soldering temperature is 290°C, although the particle shape of the solder joints disappears completely, the thickness of the solder joint begins to be uneven, which causes the chip's position relative to the substrate to tilt. This will lead to uneven distribution of the light emitting angle of the flip-chip LED filament in practical applications.

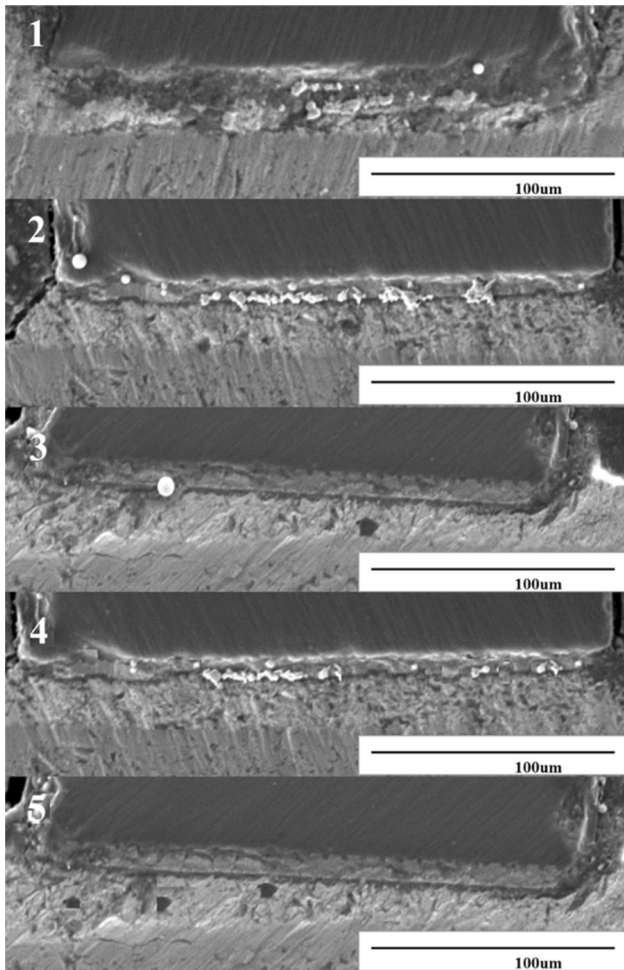


Fig. 12. The microscopic morphology of the solder joint interface of flip chip LEDs after welding at different temperatures (1) 250°C (2) 260°C (3) 270°C (4) 280°C (5) 290°C.

The voids in the chip connection solder usually cause a local increase in mechanical stress (stress concentration), and the viscoplastic deformation of SAC alloy is much higher than other areas. Fatigue cracks are easy to initiate and propagate near these high stress areas. When the temperature of the working environment changes, the solder joint will undergo irreversible plastic deformation, which will cause internal crack damage, repeatedly forming a vicious circle, and finally cause the solder joint to break and completely destroy the solder joint. Huang et al.⁴¹ analyzed the evolution of solder micro-defects in accelerated aging experiments through experiments and finite element (FE) simulations, and discussed the physical causes of die connection failures in IGBTs. The results show that voids, Sn-Ag-Cu (SAC) alloy cracks and Si/SAC interface detachment are the three main micro-defects in chip connection solder, and voids can accelerate the development of the other two micro-defects.

Figure 12 shows the microscopic morphology of the cross-sections of the solder joints of flip-chip LED chips at different soldering temperatures, where the total thickness of the metal compound IMC layer is about 2–4 μm through the test. Among them, when the welding temperature is 270°C, the IMC thickness of the solder joint cross section is the smallest. According to reports,⁴² when a thick IMC layer is formed at the interface, the reliability of the interface between the solder and the substrate will decrease. It is speculated that this phenomenon is related to the decrease of interface bonding area. And, the resistance will gradually increase as the IMC layer in the solder joint increases. This is because the internal structure of the solder matrix improves the electrical path.

Photoelectric and Thermal Properties of FC-LED LED Filament

Figure 13 shows the steady-state voltage of the FC-LED LED filament after 15 min of lighting. We

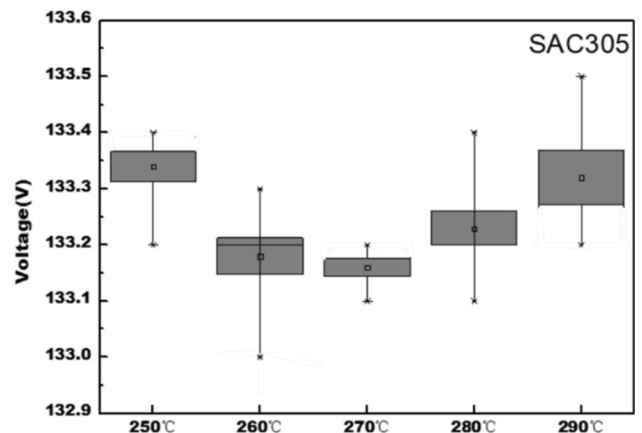


Fig. 13. The steady-state voltage of the FC-LED LED filament at different soldering temperatures.

can clearly see that the voltage of the LED filament welded at 270°C is lower than the voltage of the LED filament at other soldering temperatures. The detailed data shows that the average steady-state voltage of the LED filament at the five soldering temperatures is about 133.34 v, 133.18 v, 133.16 v, 133.24 v, 133.32 v, 133.32 v, respectively. Higher voltage will accelerate the aging rate and reduce the service life. There are more voids and cracks in the LED filament solder joints at other soldering temperatures compared with the LED filament at the 270°C soldering temperature. In addition, the contact area between the solder paste of the solder joint and the FC-LED at a soldering temperature of 270°C is larger, and the thermal resistance and steady-state voltage are smaller.¹⁴

Figure 14 shows the average junction temperature of FC-LED LED filaments at different soldering temperatures. The average junction temperature of the LED filament at the five soldering temperatures is about 75.67°C, 75.17°C,

73.23°C, 73.78°C, 75.65°C, respectively. The average junction temperature of the LED filament at a soldering temperature of 270°C is 3.33% lower than the average junction temperature of the LED filament at a soldering temperature of 250°C, and 8.21% lower than the average junction temperature of the LED filament at a soldering temperature of 290°C. The steady-state voltage increases continuously with the increase of resistance. Semiconductor devices with higher thermal resistance have poor thermal conductivity and poor heat dissipation performance. The junction temperature can be calculated by the thermal resistance formula:

$$R_{th} = \frac{L}{K \cdot S} \quad (2)$$

where L is the path length of the solder joint heat conduction, K is the thermal conductivity of the lead-free solder, and S is the cross-sectional area of the solder joint heat conduction.

Because there are more cracks in the solder joints of the LED filament at other soldering temperatures, the thermal resistance of the LED filament is higher than that at the soldering temperature of 270°C. Compared with the LED filament at the soldering temperature of 270°C, the LED filament at other soldering temperatures has a higher steady-state voltage, which has a negative impact on the service life and reliability of the FC-LED filament. The high contact resistance due to the large void ratio is considered to be the main factor that causes the chip temperature to rise.⁴³

Figure 15 shows the average blue light flux and average luminous efficiency of five LED filaments at different soldering temperatures after being lit for 30 min. Among them, the blue flux and luminous efficiency of the LED filament at a soldering temperature of 270°C are higher than those at other soldering temperatures. Figure 13 shows that the steady-state voltage of the LED filament at other soldering temperatures is higher than that of the

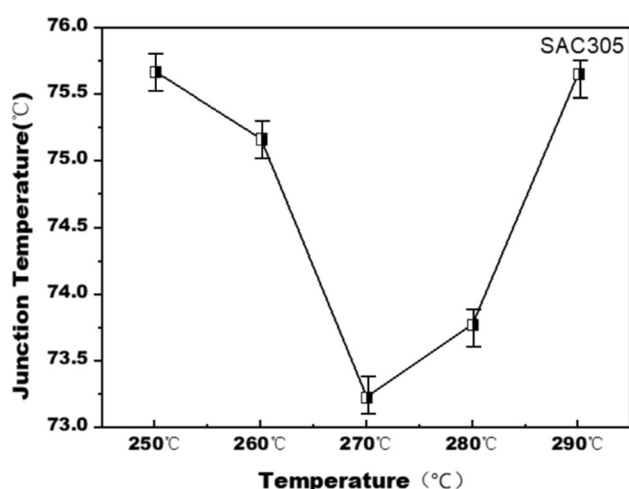


Fig. 14. The average junction temperature of FC-LED filaments at different soldering temperatures.

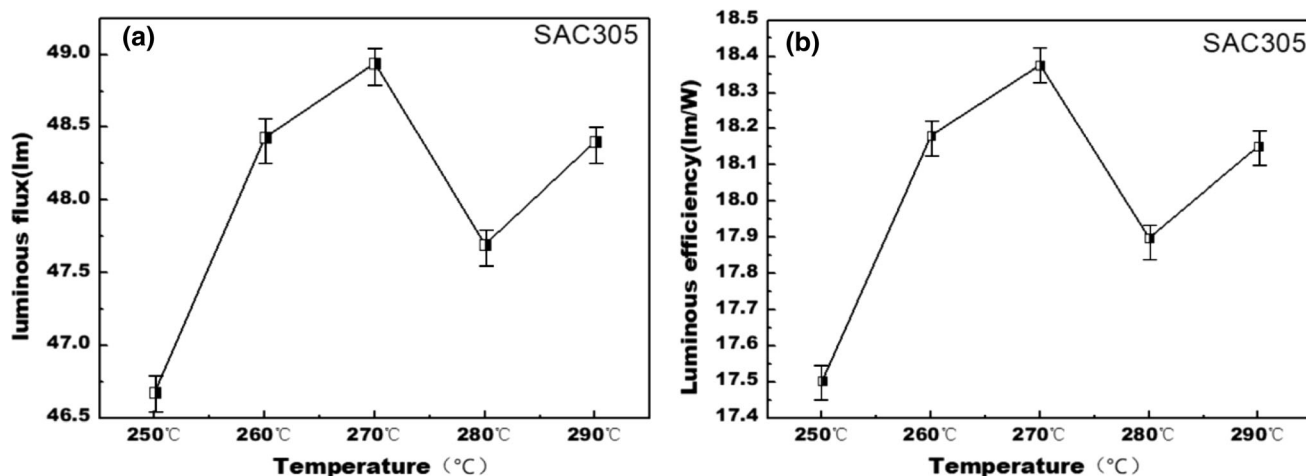


Fig. 15. Optical properties of FC-LED filaments at different soldering temperatures: (a) average blue light flux (b) average luminous efficiency.

LED filament at the soldering temperature of 270°C, and it has lower blue light flux, light efficiency and higher thermal resistance. The current density of the FC-LED filament will be reduced due to the higher thermal resistance, which directly causes the luminous flux and luminous efficiency of the LED filament to decrease.⁴⁴ In short, the LED filament welded at 270°C has a longer life, higher reliability, and higher blue light flux, light efficiency, lower steady-state voltage and higher shear strength than LED filaments at other soldering temperatures. Luo and others^{45,46} have made further research on improving the enhancement of luminous efficiency.

Analysis of Soldering Joint Fracture Mode at Different Soldering Temperatures

The steady-state voltages of five types of FC-LED filaments are shown in Table III. Under high temperature and high humidity (85°C/85%RH) aging conditions, the steady-state voltage of the five types of LED filaments decreases before aging 300 h, and then increases. In the initial stage of aging, the test environment is room temperature. When the high temperature and high humidity of the aging environment is changed to normal temperature, an

Table III. Steady state voltage (V) of LED filament after high temperature and high humidity aging

Times	250°C	260°C	270°C	280°C	290°C
0	133.34	133.18	133.16	133.23	133.32
100	132.32	132.17	132.09	132.17	132.99
200	131.67	131.53	131.43	131.89	132.78
300	132.45	132.07	131.89	131.79	132.07
400	132.38	131.99	131.76	132.31	132.56
500	131.89	132.14	131.97	132.34	132.82
600	131.76	132.23	132.08	132.23	132.78

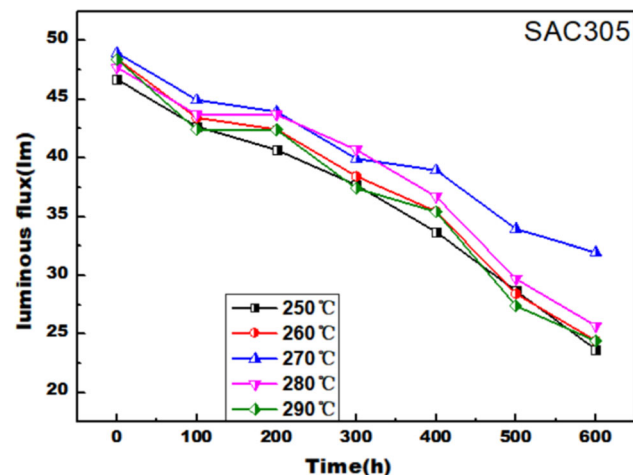


Fig. 16. Blue light flux of the LED filament after high soldering temperature and high humidity aging.

effect equivalent to the annealing effect is observed, and the defects in the solder joint are repaired to a certain extent. In general, the resistance of the LED filament decreases and the steady-state voltage decreases. However, as the aging time increases, the higher temperature damages the surface of the flip chip, resulting in deterioration of the contact between the chip and the electrode. The internal delamination of the flip chip and the solder joint intensifies, which leads to an increase in electrical resistance and poor thermal conductivity.⁴⁷ The steady-state voltage of the LED filament increases, and the overall stability decreases. The decrease of the material properties inside the chip leads to a decrease in the blue light flux.

The blue light fluxes of the five LED filaments are shown in Fig. 16. It can be observed that the blue light flux decreases after 600 h aging. The factors that accelerate the aging of FC-LED filaments are high temperature and high humidity. The aging mechanism of the LED filament lies in the acceleration of the chemical reaction at high temperature and the diffusion of moisture in the FC-LED filament caused by high humidity, thereby accelerating the aging of the LED filament. In addition, aging will change the material properties, which will cause chip corrosion and failure, and reduce the blue light flux of the LED filament.⁴⁸ In short, when the soldering temperature is 270°C, the LED filament performs better in maintaining the blue light flux.

CONCLUSIONS

In this paper, the void ratio of the flip-chip LED filament solder joint at 250°C, 260°C, 270°C, 280°C, 290°C reflow soldering temperature was detected by x-ray detector. The shear test is carried out to evaluate the influence of the interface reaction on the mechanical reliability of the solder joint, and the void distribution of the shear section is observed through the scanning electron microscope (SEM). Finally, the photoelectric and thermal performance of the FC-LED filament and the influence of high temperature and high humidity aging on the reliability of the LED filament are tested and analyzed. The specific conclusions are as follows:

- At a soldering temperature of 270°C, the voids of the solder joints are the lowest, and most of them are small voids with relatively uniform distribution. Even distribution of small voids in the joint cavity can appropriately increase its mechanical reliability.
- As the void density in the solder joint decreases, the shear strength of the solder joint increases. Since the bonding strength of the solder joint is related to the area, the reduction of the connection area and the large voids between the solder joints result in a decrease in strength. In addition, voids in the solder joint can cause stress concentration, and these

stress concentration locations are the initial part of the crack under environmental load.

- (c) A higher LED filament voltage will accelerate the aging rate and reduce the service life. There are more voids and cracks in the LED filament solder joints at other soldering temperatures compared with the LED filament at the 270°C soldering temperature. In addition, the solder paste of the LED filament solder joints soldered at 270°C has a larger contact area with the FC-LED, which has a longer life and higher reliability than the LED filament at other soldering temperatures. And it has higher blue light flux, light efficiency, lower steady-state voltage and higher shear strength.

- (d) When the soldering temperature is 270°C, the LED filament performs better in maintaining blue light flux. In the high-temperature and high-humidity aging environment, the steady-state voltage of the LED filament first decreases and then increases, which repairs the defects in the solder joint to a certain extent. As the aging time increases, the internal delamination of the flip chip and the solder joint intensifies, which causes the overall stability of the LED filament to decrease.

It can be seen from the conducted tests that the soldering temperature has an effect on the void ratio, shear stress, mechanical reliability and photoelectric thermal performance of the solder joints of flip-chip LED chips. Further design studies have been planned to analyze the shear stress and thermal properties of the weld joint through finite element simulation. In the future, we will study the influence of different grain sizes and thicknesses of the solder joint on the shear stress and micro-morphology.

ACKNOWLEDGMENTS

This research is supported by Shanghai Alliance Plan (LM201978), the Science and Technology Planning Project of Zhejiang Province, China (2018C01046), Enterprise-funded Latitudinal Research Projects (J2016-141), (J2017-171), (J2017-293), (J2017-243).

CONFLICT OF INTEREST

The authors declare that they have no conflict of interest.

REFERENCES

1. Y. Kariya, T. Hosoi, S. Terashima, and T.M. Otsuka, *J. Electron. Mater.* 33, 321 (2004).
2. M.G. Cho, S.K. Kang, and S.H.M. Lee, *J. Electron. Mater.* 36, 1501 (2007).
3. I.E. Anderson and J.L. Harringa, *J. Electron. Mater.* 33, 1485 (2004).
4. K.W. Moon, W.J. Boettinger, U.R. Kattner, F.S. Biancianiello, and C.A. Handwerker, *J. Electron. Mater.* 29, 1122 (2000).
5. Z. Guo, X. Wang, Y. Liu, Y. Liu, and F. Li, *J. Constr. Steel Res.* 172, 106174 (2020).
6. H. Yongle, L. Yifei, X. Fei, L. Binli, and T. Xin, *Microelectron Reliab.* 109, 113637 (2020).
7. K.S. Kim, S.H. Huh, and K. Sugauma, *J. Alloys Compd.* 352, 226 (2003).
8. C. Ming, C. Lung, and Lin, *J. Electron. Mater.* 32, 1426 (2003).
9. L. Yang, J. Ge, Y. Zhang, J. Dai, and Y. Jing, *J. Mater. Sci. Mater. Electron.* 26, 613 (2015).
10. S. Lei and Z. Liang, *Adv. Mater. Sci. Eng.* 2015, 1 (2015).
11. L.L. Liou, B. Bayraktaroglu, and C.I. Huang, *Solid-State Electron.* 39, 165 (1996).
12. L. Ciampolini, M. Ciappa, and P. Malberti, *Microelectron. J.* 30, 1115 (1999).
13. J. Chengshuo, F. Jiajie, Q. Cheng, Z. Hao, F. Xuejun, G. Weiling, and Z. Guoqi, *IEEE Trans. Compon. Packag. Manuf.* 99, 1 (2018).
14. Y. Liu, S.Y.Y. Leung, J. Zhao, C.K.Y. Wong, C.A. Yuan, G. Zhang, F. Sun, and L. Luo, *Microelectron. Reliab.* 54, 2028 (2014).
15. L. Hailong, A. Rong, W. Chunqing, T. Yanhong, and J. Zhi, *Mater. Lett.* 144, 97 (2015).
16. D. Bušek, K. Dušek, D. Růžička, M. Plaček, P. Mach, J. Urbánek, and J. Starý, *Microelectron. Reliab.* 60, 135 (2016).
17. T.C. Liu, C.M. Liu, Y.S. Huang, C. Chen, and K.N. Tu, *Scr. Mater.* 68, 241 (2013).
18. K. Weinberg, T. Böhme, and W.H. Müller, *Comput. Mater.* 45, 827 (2009).
19. S.K. Tippabhotla, I. Radchenko, K.N. Rengarajan, G. Illya, V. Handara, M. Kunz, N. Tamura, and A.S. Budiman, *Procedia Eng.* 139, 123 (2016).
20. Giro and A. Violeta, *Compr. Anal. Chem.* 75, 153 (2017).
21. T. Tian, K. Chen, A.A. Macdowell, D. Parkinson, Y.S. Lai, and K.N. Tu, *Scr. Mater.* 65, 646 (2011).
22. P. Wild, D. Lorenz, T. Grözinger, and A. Zimmermann, *Microelectron Reliab.* 85, 163 (2018).
23. M. Rauer, A. Volkert, T. Schreck, S. Härter, and M. Kaloudis, *J. Fail. Anal. Prev.* 14, 272 (2014).
24. A.S. Budiman, H.A.S. Shin, B.J. Kim, S.H. Hwang, H.Y. Son, M.S. Suh, Q.H. Chung, K.Y. Byun, N. Tamura, and M. Kunz, *Microelectron. Reliab.* 52, 530 (2012).
25. K.C. Otiaba, R.S. Bhatti, N.N. Ekere, S. Mallik, M.O. Alam, E.H. Amalu, and M. Ekpu, *Microelectron. Reliab.* 52, 1409 (2012).
26. M.I. Okereke and L. Yuxiao, *Appl. Therm. Eng.* 142, 346 (2018).
27. S. Baricordi, G. Calabrese, F. Gualdi, V. Guidi, M. Pasquini, L. Pozzetti, and D. Vincenzi, *Sol. Energy Mater. Sol. Cells* 111, 133 (2013).
28. W.B. Hance and N.C. Lee, *Solder Surf. Mount Technol.* 5, 16 (1993).
29. M.A.A.M. Salleh, C.M. Gourlay, J.W. Xian, S.A. Belyakov, H. Yasuda, and S.D. McDonald, *Sci. Rep. UK* 7, 40010 (2017).
30. I.E. Anderson, B.A. Cook, J. Harringa, and R.L. Terpstra, *J. Electron. Mater.* 31, 1166 (2002).
31. C.E. Ho, R.Y. Tsai, Y.L. Lin, and C.R. Kao, *J. Electron. Mater.* 31, 584 (2002).
32. D. Goyal, T. Lane, P. Kinzie, C. Panichas, and O. Villalobos, *Electron Comp Tech Con.*, p. 732 (2002).
33. M. Yunus, K. Srihari, J.M. Pitarresi, and A. Primavera, *Microelectron. Reliab.* 43, 2077 (2003).
34. Y.W. Chang, Y. Cheng, F. Xu, L. Helfen, T. Tian, M. Di Michiel, C. Chen, K.N. Tu, and T. Baumbach, *Acta Mater.* 117, 100 (2016).
35. J.M. Song, H.Y. Chuang, and Z.M. Wu, *J. Electron. Mater.* 36, 1516 (2007).
36. A.K. Gain, T. Fouzder, Y.C. Chan, and W.K.C. Yung, *J. Alloys Compd.* 509, 3319 (2011).

37. X.X.X. Xiaoqiang, Z.J.Z. Jianwei, C.J.C. Jonghyun, and C.M.C. Myungkee, *IC Electron. Packag. Technol.* (2011). <https://doi.org/10.1109/ICEPT.2011.6066934>.
38. G. Chen, X.H. Wang, J. Yang, W.L. Xu, and Q. Lin, *Microelectron. Reliab.* 108, 113634 (2020).
39. K. Mehrabi, F. Khodabakhshi, E. Zareh, A. Shahbazkhan, and A. Simchi, *J. Alloys Compd.* 688, 143 (2016).
40. C.M.T. Law, C.M.L. Wu, D.Q. Yu, L. Wang, and J.K.L. Lai, *J. Electron. Mater.* 35, 89 (2006).
41. Z. Huang, P. Kumar, I. Dutta, J.H.L. Pang, and R. Sidhu, *Eng. Fract. Mech.* 131, 9 (2014).
42. C.J. Lee, K.D. Min, H.J. Park, and S.B. Jung, *J. Alloys Compd.* 820, 153077 (2020).
43. L. Lin, Z.Z. Chen, H.P. Pan, S.L. Qi, P. Liu, Z.X. Qin, T.J. Yu, B. Zhang, Y.Z. Tong, and G.Y. Zhang, *Phys. Status Solidi-R* 4, 2834 (2007).
44. Y.T. Chin, P.K. Lam, H.K. Yow, and T.Y. Tou, *J. Mater. Res.* 25, 1304 (2010).
45. X. Luo, R. Hu, S. Liu, and K. Wang, *Prog. Energy Combust.* 56, 1 (2016).
46. X. Yu, L. Xiang, N. Pei, S. Zhou, and X. Luo, *IEEE Trans. Electron. Device* 67, 3655 (2020).
47. C. Morando, O. Fornaro, O. Garbellini, and H. Palacio, *Procedia Mater.* 1, 80 (2012).
48. G.J. Jeong, H.D. Yoo, K.K. Kim, and S.N. Lee, *J. Vac. Sci. Technol. B* 33, 051205 (2015).

Publisher's Note Springer Nature remains neutral with regard to jurisdictional claims in published maps and institutional affiliations.